DOI: 10.1002/chem.200800008

Synthesis, Characterization, and Field-Effect Transistor Properties of Carbazolenevinylene Oligomers: From Linear to Cyclic Architectures

Yabin Song,[a, b] Chong-an Di,[a, b] Zhongming Wei,[a, b] Tianyue Zhao,[a, b] Wei Xu,*[a] Yunqi Liu,*[a] Deqing Zhang,[a] and Daoben Zhu*[a]

Abstract: Two cyclic carbazolenevinylene dimers **1** and **2** were synthesized by McMurry coupling reactions. A linear compound **3** was also prepared for comparison. Compounds **1**–**3** were fully characterized by means of NMR spectroscopy, HRMS, elemental analysis, and UV/Vis absorption spectroscopy. Quantum chemical simulations showed that the cyclic compounds possessed smaller HOMO–LUMO gaps and more extended conjugation. The UV/Vis absorption spectra of the cyclic compounds showed blueshifts compared with that of the linear compound **3**. Time-dependent DFT (TD-DFT) analysis revealed that this was due to the different selection rules for molecules with cyclic and linear architectures. The cyclic conformation also significantly affected the molecular ordering in the solid state. The X-ray crystal structure of **1** showed partial π–π overlapping between the adjacent molecules. Thin films of **1**–**3** were fabricated by the vacuum-deposition method on Si/SiO_2 substrates. Multicrystalline thin films were obtained from compounds **1** and **2**, but only amorphous thin films could be obtained for the linear compound **3**. Another important difference between the cyclic and linear compounds was the reduced reorganization energy for the cyclic compounds. These two facts have resulted in improved field-effect transistor (FET) mobilities for the cyclic compounds compared with the linear compound. In addition, as the substrate temperature has a significant influence on the morphology and the degree of crystallinity of the thin films deposited, the device performance could be optimized by varying the substrate temperature. The FET devices based on **2** gave the highest mobility of $0.013\ cm^2V^{-1}s^{-1}$. The results showed that carbazole derivatives with cyclic structures might make better FETs.

Keywords: cyclooligomerization · density functional calculations · films · semiconductors · structure–activity relationships

Introduction

Organic semiconductors have been the focus of intense investigation for the past decade because of their potential electronic applications.[1] Due to their capability of transporting charge, organic semiconductors can act as active layers instead of traditional silicon in field-effect transistors (FETs).[2] Furthermore, organic materials possess many advantages over silicon, such as low cost, flexibility, and easier tailoring of the functional properties of the materials by modification of their molecular structures.[2] Some organic semiconductors may be deposited by low temperature solution processing, which allows industrial methods, such as spin coating, printing and stamping to be used.[3] Therefore, they provide alternative approaches towards the realization of low cost electronics. To date, significant progress has been made in increasing the performance of organic semiconductors in FETs in all respects of charge-carrier mobility, on/off ratio, and stability.[2,4] However, it is still a major challenge to understand the relationship between molecular structures and properties, and there are no definite guidelines for molecular designs to facilitate the charge transport.[5]

Carbazole-based materials have been widely studied for their unique electrical and optical properties.[6] They have

[a] Y. Song, C.-a. Di, Z. Wei, T. Zhao, Dr. W. Xu, Prof. Y. Liu, Prof. D. Zhang, Prof. D. Zhu
CAS Key Laboratory of Organic Solids
Beijing National Laboratory for Molecular Sciences
Institute of Chemistry, Chinese Academy of Sciences
Beijing 100080 (China)
Fax: (+86) 10-6256-9349
E-mail: wxu@iccas.ac.cn
liuyq@iccas.ac.cn
zhudb@iccas.ac.cn

[b] Y. Song, C.-a. Di, Z. Wei, T. Zhao
Graduate School of the Chinese Academy of Sciences
Beijing 100080 (China)

been used as hole-transporting materials in a variety of fields, such as organic photoconductors,[6] organic light-emitting diodes,[7] and nonlinear optics[8]. Due to their excellent hole transporting characteristics and air-stability, carbazole derivatives have also been used in FETs.[2d,9] Recently, Drolet et al. fabricated organic FETs based on thin films of 2,7-carbazolenevinylene-based oligomers and obtained high hole mobilities ($0.3\ cm^2 V^{-1} s^{-1}$).[9d] Ong and co-workers have also reported a series of indolo[3,2−b]carbazole derivatives that can be used to fabricate high-mobility FETs under ambient conditions.[9b,c] This research indicates that carbazole-based materials can be attractive candidates for FET applications.

Conjugated macrocyclic oligomers have become a topic of growing interest in several fields of research, including supramolecular chemistry, organic materials science, and nanotechnology.[10] The cyclic structure of these compounds represents a defect-free and well-defined π-conjugated chain, which ideally combines an infinite polymer with the structural features of a well-defined oligomer, but without any perturbing end-effects.[11] Cyclic oligomers based on carbazole have been synthesized and investigated.[12] Importantly, several carbazolylacetylene-derived macrocycles have been reported that have unique fluorescence-quenching-based chemical detection,[13] self-assembly,[14] and photoinduced charge-transfer properties.[15] However, their synthesis is always complicated, and their potential use in FETs has been scarcely studied so far. Furthermore, comparing the properties of the cyclic oligomers with those of the linear oligomers will provide useful information for molecular design in the development of novel molecular materials.

Based on previous work on the synthesis of the triphenylamine dimer and carbazolylacetylene-derived macrocycles,[15,16] we planned to apply the McMurry reaction for the synthesis of cyclic carbazolenevinylene oligomers. Carbazole units were linked by two ethylene groups resulting in two cyclic dimers (compounds **1** and **2**). The introduction of carbon–carbon double bonds in organic conductors is deemed to reduce the band gap and tune the electrical properties with an extended π-conjugated length.[9d,17] For comparison, a linear carbazole dimer (compound **3**) was also synthesized. The optical and electronic properties of **1**–**3** were fully characterized. To investigate their hole-transporting properties, FET devices were fabricated and tested in detail. They all worked as *p*-type semiconductors. The film morphologies and molecular structures were discussed in relation to the device performances.

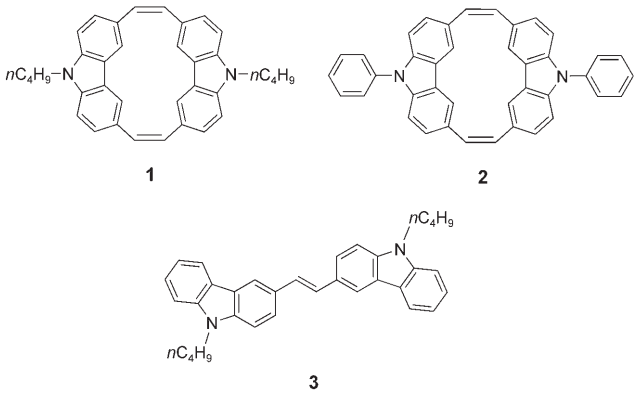

1 2 3

Results and Discussion

Synthesis: The procedure for the synthesis of compounds **1**–**3** is shown in Scheme 1. Compounds **1** and **2** were synthesized by a similar process to that we have reported previously.[16] Two formyl groups were introduced into carbazole to give the precursor of **1** in high yield by direct Vilsmeier–Haack formylation employing DMF and phosphorus oxychloride.[18] However, for phenyl-substituted carbazole **6**, the yield was very low. Thus, **6** was brominated, followed by

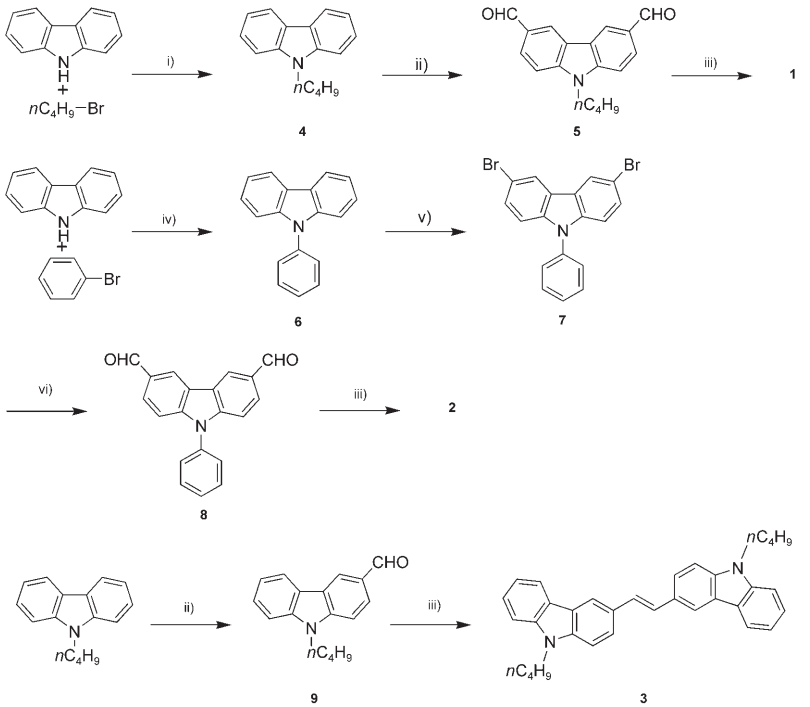

Scheme 1. i) TBAI, NaOH; ii) $POCl_3$, DMF; iii) $TiCl_4$, Zn, pyridine, 80 °C; iv) K_2CO_3, CuI, [18]crown-6; v) NBS; vi) −78 °C, *n*BuLi, DMF. TBAI = tetrabutylammonium iodide; NBS = *N*-bromosuccinimide

lithiation and reaction with DMF, which afforded the diformyl compound **8** in a satisfactory yield. Compounds **1–3** were realized by McMurry coupling reactions.[16,19] The reactions of 9-*n*-butyl-carbazole-3,6-dicarbaldehyde and 9-phenyl-carbazole-3,6-dicarbaldehyde with $TiCl_4$, Zn powder, and pyridine in THF at reflux under nitrogen gave **1** and **2** in yields of 8.1 and 5.6%, respectively. Although the yields were low, the syntheses were simple and could be operated on a large scale. Compound **3** was also synthesized by McMurry reactions in 58.0% yield. Compounds **1** and **3** were soluble in common organic solvents, such as dichloromethane and toluene, with a high solubility ($>10\,mg\,mL^{-1}$), but **2** had very low solubility in organic solvents ($<1\,mg\,mL^{-1}$ in chloroform or toluene at room temperature). All compounds were characterized by HRMS, NMR spectroscopy, and elemental analysis. Compound **2** could not be characterized by ^{13}C NMR spectroscopic analysis due to its poor solubility. Thermogravimetric analysis (TGA) measurements gave thermal decomposition temperatures (T_d) of 466, 406, and 420°C for **1**, **2**, and **3**, respectively. Their melting points were all above 200°C, which showed that they all possessed excellent thermal stability.

Crystal structure: Single crystals of **1** for X-ray analysis were obtained by slow evaporation of its dichloromethane solution. The crystal belongs to a crystal system of orthorhombic space group *Pbca* with unit-cell parameters of $a=15.618(3)$, $b=8.4122(17)$, $c=19.403(4)$ Å. As shown in Figure 1a, molecule **1** has a symmetric center located at the center of the cyclic structure. The carbazole moieties band to a nonplanar comformation with a dihedral angle of about 12° between the five-membered ring and fused six-membered ring. Molecules stacked in a column along the *b*-axis can be observed when the structure is viewed along the *c*-axis (Figure 1b). There is partial π–π overlapping between the adjacent molecules in the same column, as the interplane distance between two N-hetero rings is about 3.25 Å. This column-stacking manner may favor efficient hole transportation.

Optical and electrochemical properties: The UV/Vis spectra of **1–3** in dichloromethane and in neat films are shown in Figure 2. Their spectra in solution showed absorption peaks at 298, 300, and 343 nm, respectively. In thin films prepared by the vacuum-deposition method, the absorption maxima of **1** and **2** were at 304 and 307 nm, exhibiting a small red-shift and broadening in comparison with that in solution. This indicated the formation of J-aggregates in the solid state. The spectrum of compound **3** as a film showed a smaller shift, which indicated loose congregation. From the absorption edges of the thin film spectra, optical band gaps of **1**, **2**, and **3** were estimated as 3.51, 3.21, and 2.88 eV, respectively. The band gaps in **1** and **2** were much larger than in the linear analogue **3**, which showed that they might be more stable. This is in conflict with the HOMO–LUMO gaps (HLGs) obtained from the quantum simulation, which is discussed below.

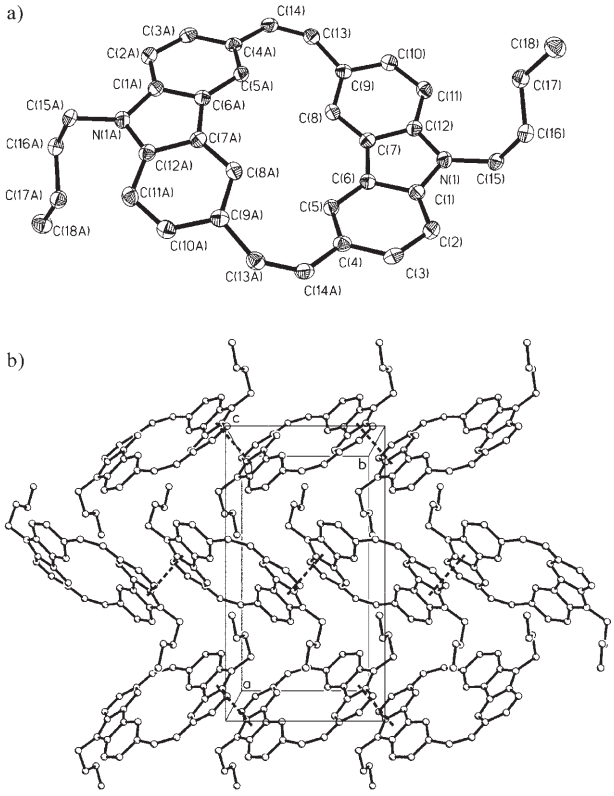

Figure 1. a) Molecular structure of compound **1** with 50% possibility ellipsoids. b) Stacking pattern of **1** in the crystal view along the *c*-axis, intermolecular π–π interactions are indicated by ----- (hydrogen atoms were omitted for clarity).

Cyclic voltammetric measurements have been carried out on compounds **1–3**. We used a conventional three-electrode cell with Pt working electrodes, a platinum wire counter electrode, and an Ag/AgCl reference electrode at room temperature. The experiments were calibrated with the ferrocene/ferrocenium (Fc/Fc^+) redox system. They all showed two reversible oxidation waves corresponding to the oxidation of each of the nitrogens (Figure 3). The two oxidation peaks of **1** were found at 0.804 and 1.079 V (vs. Ag/AgCl), whereas **2** had peaks at 0.928 and 1.142 V. They were all a little higher than the potentials of **3** (0.791, 1.128 V). The large separation of the redox potentials indicated that the two carbazole units were strongly electronically coupled. We used the onset oxidation potentials to determine the HOMO levels based on the internal standard ferrocene value of −4.8 eV with respect to the zero vacuum level.[20] The HOMO levels could be estimated by using the equation $HOMO=-(E_{ox}^{onset}+4.4)$ eV.[21] Therefore, the HOMO levels of **1–3** were estimated by using the oxidation onsets (0.69 V for **1**, 0.82 V for **2,** and 0.70 V for **3**) and were found to be −5.09, −5.22, and −5.10 eV, respectively. These values were very low, which implies high oxidative stability. The appropriate HOMO level of **1** and **3** also matched well with the work function of metallic gold (−5.1 eV). This might enhance the hole injection between the electrode and *p*-channel type semiconductor, and thus improve the device perfor-

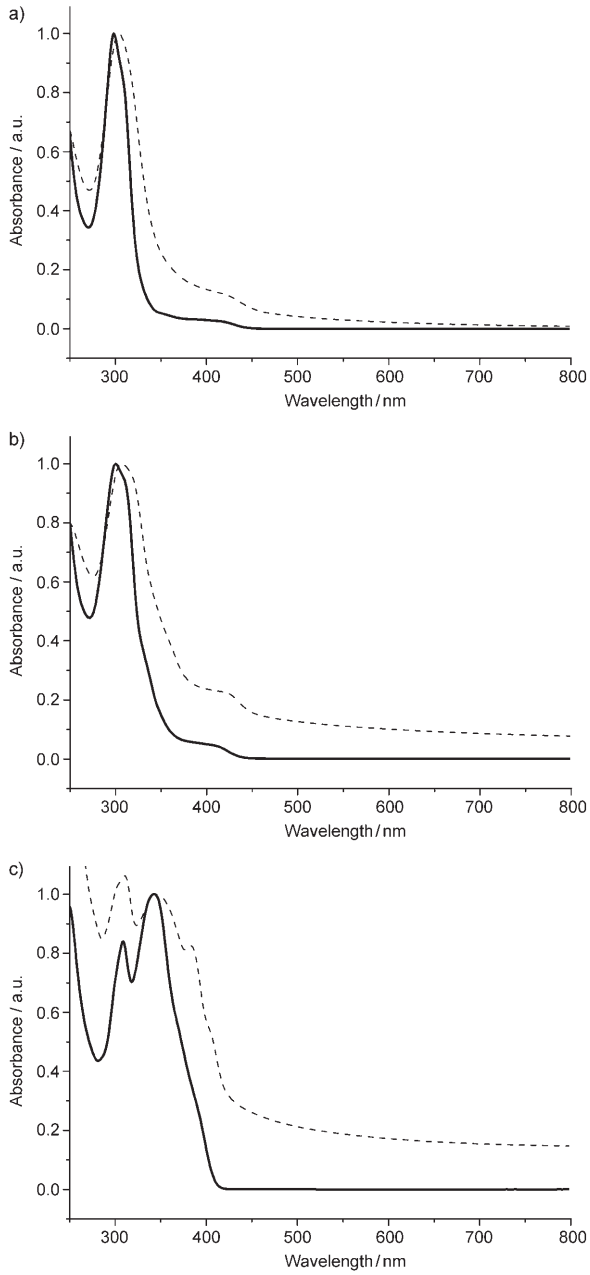

Figure 2. UV/Vis absorption spectra of a) **1**, b) **2**, and c) **3** in dichloromethane (——) and as thin films (-----). Thin films of **1**–**3** about 50 nm thick were fabricated by a vacuum-deposition method on quartz substrates at room temperature.

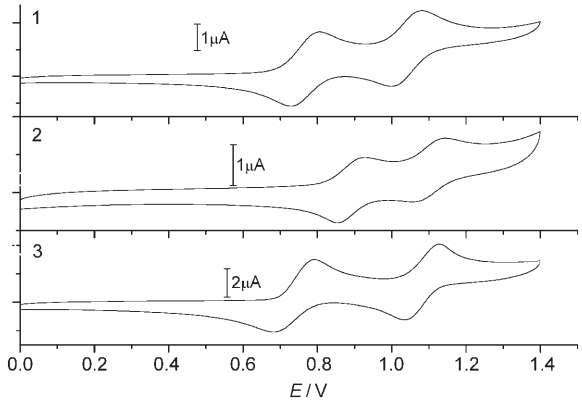

Figure 3. Cyclic voltammograms of **1**–**3** in dichloromethane at room temperature (scan rate = 50 mVs^{-1}).

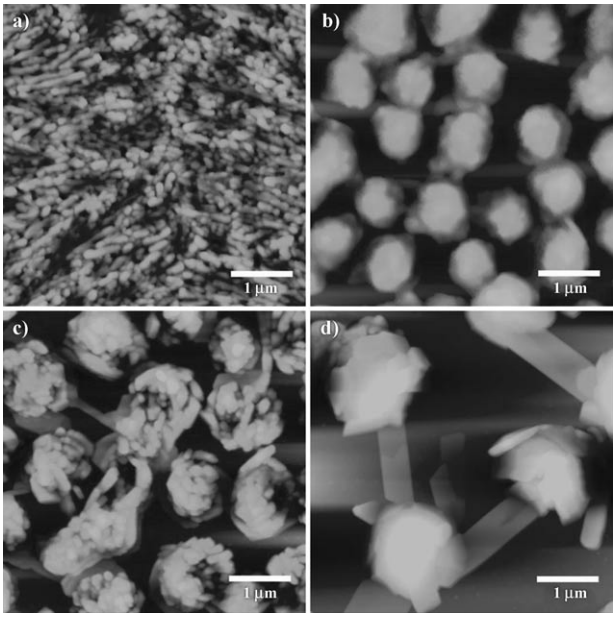

Figure 4. AFM images of the films of compound **1** on OTS treated Si/SiO_2 deposited at a) 20, b) 40, c) 60, and d) 100 °C (~50 nm thickness). Each image is 5 μm × 5 μm.

mance. On the contrary, the HOMO level of **2** was a little larger than the work function of metallic gold.

Thin films: Thin films of **1**–**3** were fabricated by a vacuum-deposition method on Si/SiO_2 substrates. The Si/SiO_2 substrate was highly n^+-doped Si with a 450 nm thermally oxidized SiO_2 layer on it. Before the deposition of the organic semiconductor, an octadecyltrichlorosilane (OTS) self-assembled monolayer was preformed on the surface of SiO_2. We used several substrate temperatures (T_{sub}) during the deposition process. Atomic-force microscopy (AFM) was used to investigate these films (Figures 4 and 5). The films of compound **1** deposited at room temperature (20 °C) showed a smoother morphology than those deposited at higher temperatures, but with a small grain size. While the grain size grew as the substrate temperature increased, the films became discontinuous bundlelike structures at 40 and 60 °C. At a substrate temperature of 100 °C, crystalline belts linking these bundles could be observed. A similar trend in film morphologies was observed for compound **2**. At a substrate temperature of 20 °C, the film was very even and continuous. The substrate was covered by the material and a good network interconnection was formed between the crystallites. When the substrate temperature increased, the films became very rough and discontinuous. At 60 °C, besides separated bundlelike structures at the film surface, a continuous smooth film could be observed underneath these bulges.

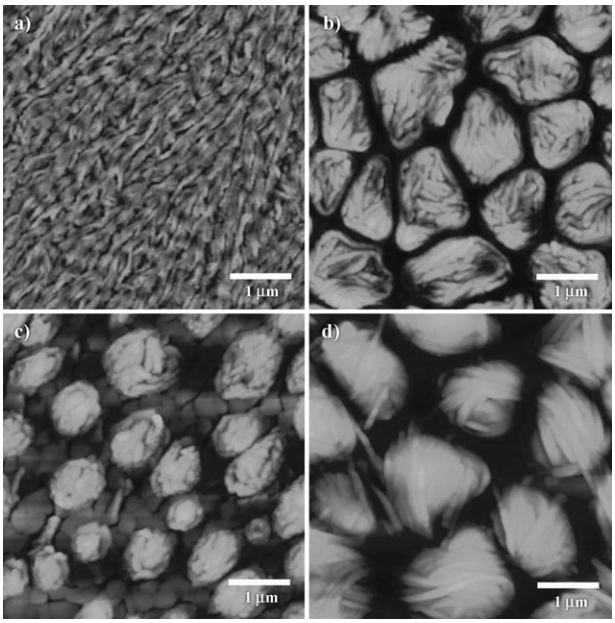

Figure 5. AFM images of the films of compound **2** on OTS treated Si/SiO_2 deposited at a) 20, b) 40, c) 60, and d) 100 °C (~50 nm thickness). Each image is 5 μm × 5 μm.

This might account for the high mobility observed at this temperature. At 100 °C, the films showed clewlike structures with bigger boundaries between the clews. For compound **3**, we fabricated thin films at room temperature (20 °C), and they showed a similar morphology to that observed for compound **2** at the same T_{sub} (Figure 6).

These films were also characterized by XRD (Figure 7). The XRD patterns of thin films of **1** exhibited weak diffraction peaks at all temperatures, and thus showed low crystallinity. Although films obtained at a substrate temperature of 40 and 100 °C showed relatively stronger diffractions than that obtained at 20 °C, they showed less continuity. This should account for the higher FET mobility observed in the films deposited at 20 °C. For compound **2**, diffraction peaks could only be observed on films deposited at 60 °C. This indicated that the films with a relatively high degree of ordering and crystallinity were formed at this temperature. The optimized thin films of **3** exhibited no XRD peaks, and thus showed amorphous properties.

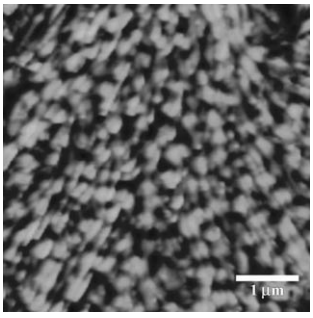

Figure 6. AFM image of a thin film of compound **3** on OTS treated Si/SiO_2 deposited at 20 °C (~50 nm thickness). The image is 5 μm × 5 μm.

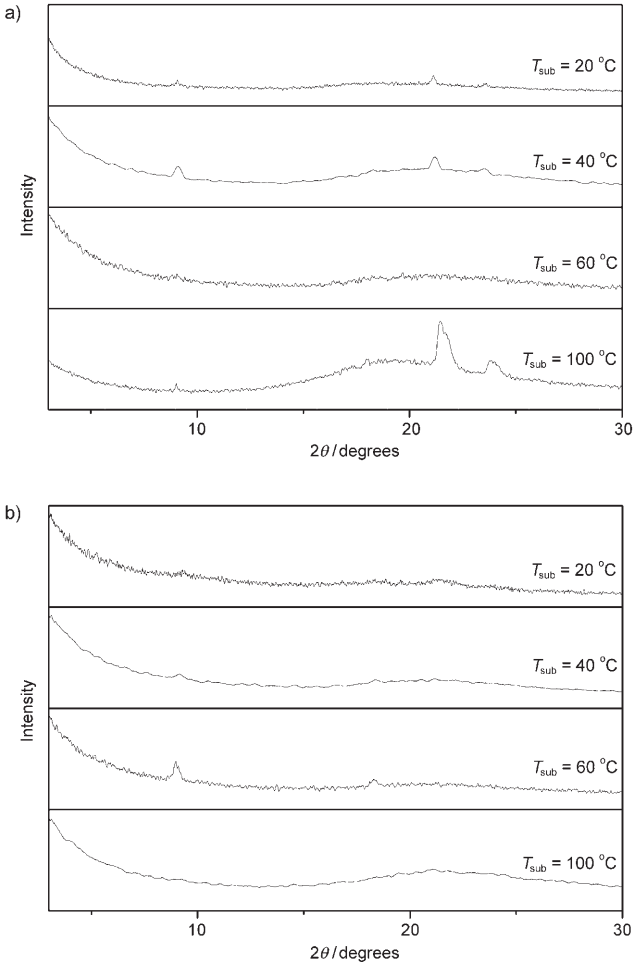

Figure 7. XRD patterns of vacuum-deposited thin films of a) **1** and b) **2** on OTS treated Si/SiO_2 substrate at various substrate temperatures (T_{sub}).

FET Measurements: FET devices were fabricated by using top-contact geometry. The thin films (~50 nm) of **1**, **2**, and **3** were deposited on OTS treated Si/SiO_2 substrates by using the vacuum-deposition method as noted above. Subsequently, gold electrodes were deposited by vacuum evaporation on the organic layer through a shadow mask. The characteristics of the FETs were obtained at room temperature in air. The mobilities were extracted in the saturation regime from the gate sweep by using Equation (1):

$$I_{DS} = (\frac{\mu W C_i}{2L})(V_G - V_T)^2 \quad (1)$$

in which I_{DS} is the drain-source current, μ is the field-effect mobility, W is the channel width, C_i is the capacitance per unit area of the gate dielectric layer, L is the channel length, and V_G and V_T are the gate voltage and threshold voltage, respectively. The FET characteristics of the devices based

on **1**–**3** at different substrate temperatures are summarized in Table 1. As examples, the output and transfer characteristics of the devices are shown in Figure 8. These compounds all displayed *p*-type accumulation FET behaviors. They all showed well-defined linear and saturation-regime output characteristics.

Table 1. The performance of FETs based on compounds **1**, **2**, and **3** prepared at different deposition temperatures of the substrate (T_{sub}).

Compound	T_{sub} [°C]	Mobility [$cm^2V^{-1}s^{-1}$]	On/Off ratio	Threshold voltage [V]
1	20	5.3×10^{-3}	10^6	−4.7
	40	2.6×10^{-4}	10^5	−28.9
	60	1.2×10^{-4}	10^4	−26.3
	100	–	–	–
2	20	1.5×10^{-4}	10^4	−20.4
	40	2.7×10^{-3}	10^6	−23.6
	60	1.3×10^{-2}	10^7	−22.0
	100	1.8×10^{-3}	10^6	−26.8
3	20	3×10^{-4}	10^4	−6.4

From Table 1, we can see that the carrier mobilities of the FETs were dependent on the substrate deposition temperatures. With the increase of T_{sub}, the mobility of compound **1** decreased. This was not surprising because film discontinuities and large gaps increased as well, which had a large negative effect on charge-transporting ability. No field effect was found at 100 °C, which may result from the discontinuity of the thin film as mentioned above. For compound **2**, the highest mobility of 0.013 $cm^2V^{-1}s^{-1}$ was measured at a T_{sub} of 60 °C. The on/off current ratio was also excellent with an order of magnitude of 10^7. This was because a more ordered thin film was formed at this temperature, which was evident from AFM and XRD. The decrease in mobility (1.8×10^{-3} $cm^2V^{-1}s^{-1}$) at a T_{sub} of 100 °C was possibly due to the large boundaries between grains.

Similar to what was observed with triphenylamine dimers of linear and cyclic architectures,[16] the FET performance of linear compound **3** was worse than that of cyclic compounds **1** and **2**. Two facts should account for such differences between the mobilities for the cyclic and linear compounds. First, the cyclic structure significantly improved the molecular ordering and π–π stacking in vapor deposited thin films. Only amorphous films could be obtained from compound **3** as indicated by XRD analysis. For compound **1** and **2** multicrystalline thin films could be prepared by the vapor evaporation method. Second, the cyclic structure led to a significant reduction in molecular reorganization energy.[16]

Quantum chemical calculations: To gain an insight into the relationship between the molecular structures and properties of these cyclic compounds, we performed quantum-chemical calculations by using the Gaussian 03 program.[27] The geometry optimization, frequency, and reorganization energy were calculated at the DFT level by using the B3LYP functional with 6-31G* basis sets. TD-DFT was used in the calculation of transition energies at the B3LYP/6-31G* level.

In the UV/Vis spectra of compounds **1**, **2**, and **3** (Figure 2), the first intensive absorptions of cyclic dimers are blueshifted by about 40 nm with respect to the linear compound. This conflicts with the HLG determined by quantum simulation. To understand such phenomena, we have calculated the transition energy by using TD-DFT. The results are collected in Table 2. The calculated maxima are in good agreement with experimental observations. It can be seen that the transition-energy differences for these compounds are due to the different assignments of these transitions, which mainly belong to HOMO−1–LUMO and HOMO–LUMO+3 transitions for the cyclic compounds and to the HOMO–LUMO transition for the linear analogue. Such different selection rules for linear and cyclic conjugated oligomers have also been noted by Bäuerle and co-workers in cyclic and linear oligothiophenes.[22]

At room temperature, the charge mobility of organic materials is often determined by a hopping transport process,[23] and two major parameters determine the charge mobility: the intermolecular electronic coupling and the reorganization integral.[24] In previous work, we found that, for a triphenylamine dimer, the reorganization energy could be significantly reduced from a linear molecule to a cyclic architecture. To validate such a structure–property relationship, we also calculated the reorganization energy for these carbazole derivatives. Similar to that observed for triphenylamine dimers, the cyclic compounds **1** and **2** possess lower reorganization energy (0.177 and 0.180 eV) compared with that of linear molecule **3** (0.275 eV). It is known that the reorganization energy is dependent on the conjugation degree.[25] From the calculated HLGs of compounds **1**, **2**, and **3**, we can see that the cyclic molecules possess lower HLGs referring to an extended conjugation in the cyclic architecture. From the difference between the bond lengths of neutral molecules and cations we can also get some clues about the trends in the reorganization energies of these carbazole derivatives. The bond length changes for compounds **1** and **3** are shown in Figure 9. It can be seen that the bond length changes upon oxidation for compound **1** are significantly smaller (average difference 0.0084 Å) than those of compound **3** (average difference 0.0172 Å). This is consistent with the reorganization energy difference between compounds **1** and **3**. In conclusion, the extended conjugation and restricted cyclic conformation have limited the conformation changes of the cyclic oligomers before and after oxidation and resulted in the reduction of the reorganization energy in comparison with that of the linear analogue.

Conclusion

We have synthesized three carbazolenevinylene oligomers by McMurry coupling reactions, the linear compound **3** and the cyclic compounds **1** and **2**. They were fully characterized by means of NMR spectroscopy, HRMS, and elemental

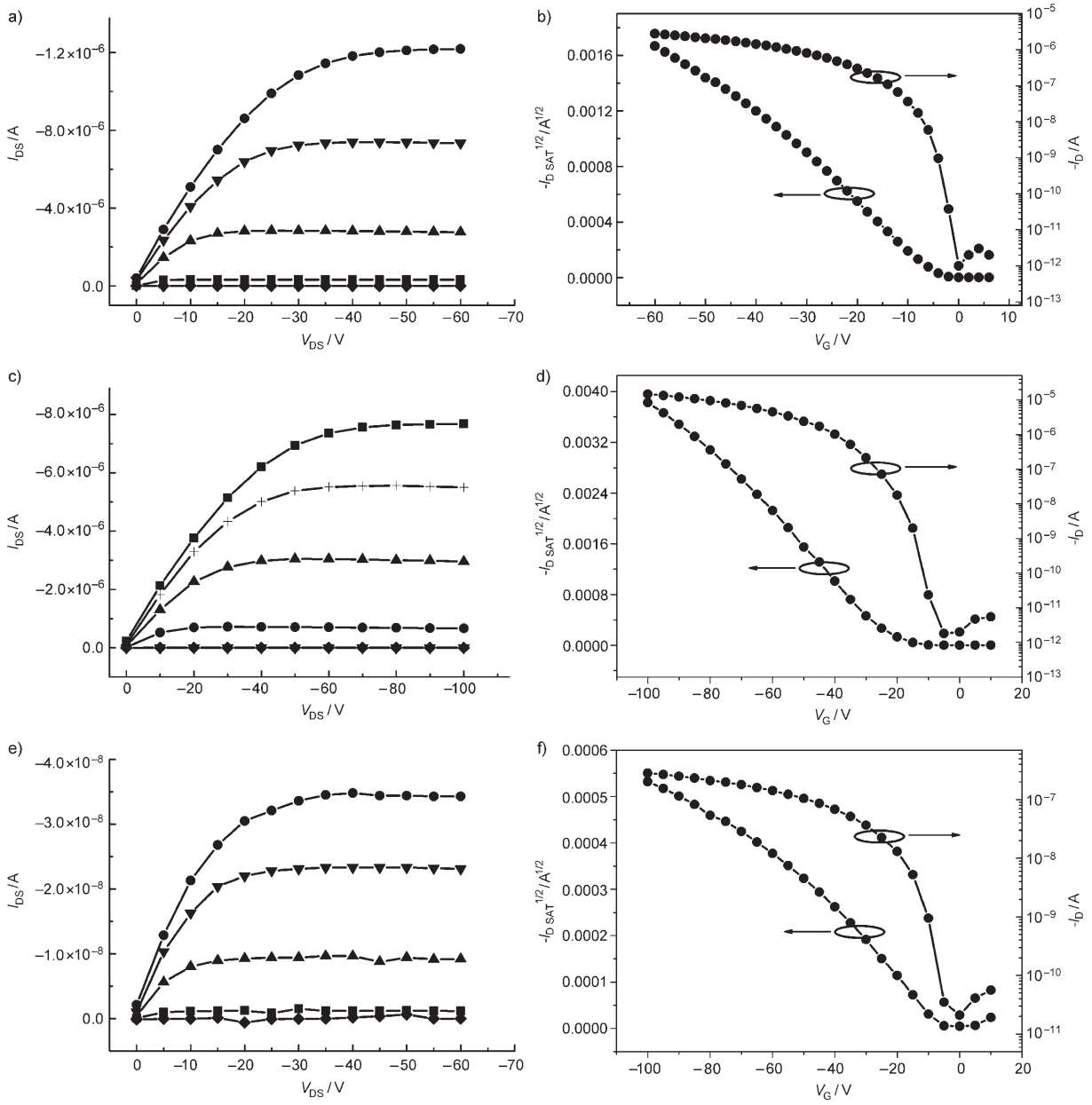

Figure 8. Plots of drain-to-source current (I_{DS}) versus drain-to-source voltage (V_{DS}) for the FET device of a) **1** at $T_{sub}=20$°C (●: −40 V, ▼: −30 V, ▲: −20 V, ■: −10 V, ◆: 0 V); b) $-I_{DS}$ and $(-I_{DS})^{1/2}$ versus V_G plots for the same device as a) at V_{DS} of −100 V; c) plots of I_{DS} versus V_{DS} for the FET of **2** at $T_{sub}=60$°C (■: −100 V, +: −80 V, ▲: −60 V, ●: −40 V, ▼: −20 V, ◆: 0 V); d) $-I_{DS}$ and $(-I_{DS})^{1/2}$ versus V_G plots for the same device as c) at V_{DS} of −100 V; e) plots of I_{DS} versus V_{DS} for the FET of **3** at 20°C (●: −40 V, ▼: −30 V, ▲: −20 V, ■: −10 V, ◆: 0 V); f) $-I_{DS}$ and $(-I_{DS})^{1/2}$ versus V_G plots for the same device as e) at V_{DS} of −100 V.

Table 2. The calculated HOMO–LUMO gap (HLG), reorganization and transition energies (λ_{max}), oscillator strengths (f), and composition of the first intense transition of compounds **1**, **2**, and **3**.

Compound	HLG [eV]	Reorganization energy [eV]	λ_{max} [nm]		f	Composition[a]
			Calcd	Exptl		
1	3.48	0.177	308.13	298	1.1162	$0.44157_{\chi(131\rightarrow133)}+0.45203_{\chi(132\rightarrow136)}$
2	3.54	0.18	337.58	300	0.6899	$0.52955_{\chi(139\rightarrow141)}+0.25805_{\chi(140\rightarrow144)}+0.28929_{\chi(140\rightarrow148)}$
3	3.82	0.275	356.68	343	0.7375	$0.53878_{\chi(126\rightarrow127)}+0.12840_{\chi(124\rightarrow127)}+0.37717_{\chi(126\rightarrow128)}$

[a] Orbital 131 is the HOMO−1 of compound **1**, orbital 139 is the HOMO−1 of compound **2**, and orbital 126 is the HOMO of compound **3**.

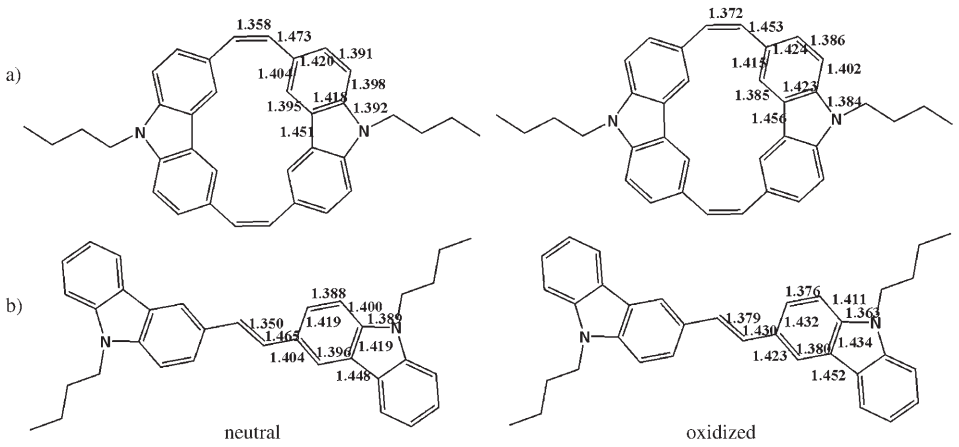

Figure 9. Bond lengths [Å] of neutral and oxidized compounds a) **1** and b) **3**.

analysis. Quantum chemical simulations showed that the cyclic compounds possessed lower HLGs and more extended conjugation. However the UV/Vis absorption spectra of the cyclic compounds showed blueshifts compared with that of linear compound **3**. TD-DFT analysis revealed that this was due to the different selection rules for molecules with cyclic and linear architectures. The cyclic conformation also significantly affected the molecular ordering in the solid state. Only amorphous thin films could be obtained from compound **3**, whereas multicrystalline thin films were obtained from compounds **1** and **2** by using the thermal evaporation method. Another important difference between these cyclic and linear compounds was the reorganization energy reduction for the cyclic compounds. These two differences resulted in improved FET mobilities for the cyclic compounds versus the linear compound. In addition, the substrate temperature has a significant influence on the morphology and the degree of crystallinity of the thin films deposited, and the device performance could be optimized by varying the substrate temperature. The FET devices based on **2** gave the highest mobility of $0.013\ cm^2V^{-1}s^{-1}$. The mobilities of devices based on **1** and **2** were higher than that of the linear compound **3**. The results showed that the carbazole derivatives with cyclic structures might fit better for FETs.

Experimental Section

General: All air/moisture-sensitive materials were handled under a nitrogen atmosphere by using Schlenk techniques. THF was distilled over sodium/benzophenone. Pyridine was distilled over NaOH. All reagents were used as received unless otherwise noted. 9-*n*-Butylcarbazole (**4**) was prepared as we have reported previously.[15] 9-Phenyl-carbazole (**6**) and 3,6-dibromo-9-phenylcarbazole (**7**) were synthesized according to literature procedures.[26] Melting points were recorded on a BÜCHI melting point B-500 apparatus. ^{1}H NMR and ^{13}C NMR spectra were obtained on Bruker Advance 300 or 400 MHz spectrometers. EIMS measurements were performed on UK GCT-Micromass or SHIMADZU G-MS-QP2010 spectrometers. HRMS measurements were performed on a Bruker APEX II FTICRMS spectrometer.

Thermogravimetric (TGA) and differential thermal (DTA) analyses were performed by using a Shimadzu DTG 60 Thermal Analyzer. A heating rate of 10 °C min^{-1} under flowing N_2 was used with runs being conducted from room temperature to 550 °C.

UV/Vis spectra were recorded on a JASCO V-570 spectrometer. Cyclic voltammetric measurements were recorded on a CHI660C voltammetric analyzer (CH Instruments, USA). They were carried out in a conventional three-electrode cell by using Pt button working electrodes of 2 mm diameter, a platinum wire counter electrode, and a Ag/AgCl reference electrode at room temperature. Conditions: 0.1 M $(n\text{Bu})_4\text{NPF}_6$ in dichloromethane.

XRD measurements of thin films were performed in the reflection mode at 40 kV and 200 mA with $Cu_{K\alpha}$ radiation by using a 2 kW Rigaku X-ray diffractometer.

AFM images of the organic thin films were obtained on a Nanoscope IIIa AFM (Digital Instruments) in tapping mode.

X-ray structures: X-ray crystallographic data were collected with a Bruker Smart CCD diffractometer by using graphite-monochromated $Mo_{K\alpha}$ radiation ($\lambda = 0.71073$ Å). The data were collected at 113 K and the structure was resolved by the direct method and refined by full-matrix least-squares on F^2 The computation was performed with the SHELXL-97 program. All non-hydrogen atoms were refined anisotropically.

Rodlike single crystals of **1** were obtained by slow evaporation of its dichloromethane solution. Crystallographic data for **1**: Crystal size: $0.12\times0.10\times0.08\ mm^3$; orthorhombic; *Pbca*; $Z=4$; $a=15.618(3)$, $b=8.4122(17)$, $c=19.403(4)$ Å; $V=2549.1(9)$ Å^3; $\rho_{calcd}=1.289\ g\,cm^{-3}$; of 14602 reflections, 2243 were unique ($R_{int}=0.0943$); GOF = 1.240; 173 parameters; $R1=0.0840$, $wR2=0.1529$ (for all reflections). CCDC 676722 contains the supplementary crystallographic data for this paper. These data can be obtained free of charge from The Cambridge Crystallographic Data Centre via www.ccdc.cam.ac.uk/data_request/cif.

Device fabrication: Thin-film transistors were made in a top-contact device configuration. Prior to the deposition, **1**–**3** were purified twice by vacuum sublimation. The substrate was highly n^+-doped Si with a 450 nm thermally oxidized SiO_2 layer on it. Before the deposition of the organic semiconductor, OTS treatment was performed on the gate dielectrics which were placed in a vacuum oven with OTS at a temperature of 120 °C to form an OTS self-assembled monolayer. Then, the treated substrates were rinsed with heptane, ethanol, and chloroform, and then dried with nitrogen. Under a base pressure of $4\sim6\times10^{-4}$ Pa, thin films of **1**, **2**, and **3** about 50 nm thick were deposited on the OTS treated Si/SiO_2 at a rate of 1 Å s^{-1}. On the surfaces of the prepared thin films, 20 nm thick gold was vacuum deposited through a shadow mask to give the source (S) and drain (D) electrodes. The channel length L was 0.05 mm and the width W was 3 mm. The FET characteristics of the devices were obtained at room temperature in air by using a Hewlett–Packard (HP) 4140B semiconductor parameter analyzer.

Quantum chemical calculations: DFT and TD-DFT calculations were carried out by using the Gaussian 03 program.[27] All geometries and electronic properties were calculated by assuming the target molecules to be isolated molecules in the gas phase.

9-*n*-Butyl-carbazole-3,6-dicarbaldehyde (5): Phosphorus oxychloride (51.56 mL, 0.553 mol) was added dropwise to DMF (43.06 mL, 0.559 mol) at 0 °C, and the mixture was stirred for 1 h at this temperature. 9-*n*-Butylcarbazole (6.624 g, 0.0297 mol) was added and the reaction mixture was stirred at 100 °C for 6 h. Then, the mixture was cooled to room temperature, poured into ice water and carefully neutralized with sodium hydroxide. The solution was extracted with dichloromethane(3×150 mL).

The organic phase was washed with water (2×100 mL) and dried over anhydrous sodium sulfate. After filtration, the solvent was removed. The crude product was purified by column chromatography on silica gel (20% CH_2Cl_2 in petroleum ether) to give **5** (6.082 g, 73.4%). ^{1}H NMR (400 MHz, $CDCl_3$): δ=10.14 (s, 2H), 8.67 (s, 2H), 8.10 (d, J=8.5 Hz, 2H), 7.57 (d, J=8.5 Hz, 2H), 4.42 (t, J=7.2 Hz, 2H), 1.95–1.87 (m, 2H), 1.48–1.38 (m, 2H), 1.00 ppm (t, J=7.3 Hz, 3H); ^{13}C NMR (100 MHz, $CDCl_3$): δ=191.19, 144.47, 129.35, 127.59, 123.81, 122.83, 109.51, 43.29, 30.75, 20.22, 13.56 ppm; MS (EI): m/z: 279 $[M]^+$; HRMS (GCT-MS): calcd for $C_{18}H_{17}NO_2$: 279.1259; found: 279.1260 $[M]^+$.

Compound 1: Zn powder (9.32 g, 143 mmol) was suspended in THF (200 mL) under N_2. A solution of $TiCl_4$ (7.76 mL, 71.6 mmol) in CH_2Cl_2 (50 mL) was added carefully to the suspension with stirring and then the suspension was heated to reflux at 80°C for 1 h. A solution of **5** (2 g, 7.17 mmol) and pyridine (5 mL) in THF (100 mL) was added dropwise to the reaction mixture. The mixture was stirred and heated at reflux for 10 h, and after cooling to room temperature, saturated aqueous $NaHCO_3$ (200 mL) was added and the reaction mixture was stirred for a further 0.5 h. The reaction mixture was filtered and most of the filtrate was removed under reduced pressure. The residual mixture was extracted with dichloromethane(3×100 mL) and the combined organic extracts were dried over anhydrous sodium sulfate, filtered, and concentrated under reduced pressure. The residue was purified by flash chromatography on silica gel (20% CH_2Cl_2 in petroleum ether) to afford the crude product. Recrystallization from CH_2Cl_2/hexane gave **1** as a yellow powder (135 mg, 8.1%). M.p. 260°C; ^{1}H NMR (400 MHz, $CDCl_3$): δ=9.79 (s, 4H), 7.25–7.18 (m, 8H), 6.36 (s, 4H), 4.20 (t, J=7.1 Hz, 4H), 1.90–1.82 (m, 4H), 1.49–1.40 (m, 4H), 1.00 ppm (t, J=7.3 Hz, 6H); ^{13}C NMR (100 MHz, $CDCl_3$): δ=140.85, 129.71, 128.08, 127.75, 123.54, 119.93, 108.78, 42.86, 30.95, 20.43, 13.77 ppm; MS (EI): m/z: 494 $[M]^+$; HRMS (GCT-MS): calcd for $C_{36}H_{34}N_2$: 494.2722; found: 494.2720 $[M]^+$; elemental analysis calcd (%) for $C_{36}H_{34}N_2$: C 87.41, H 6.93, N 5.66; found: C 87.19, H 7.01, N 5.80.

9-Phenyl-carbazole-3,6-dicarbaldehyde (8): A hexane solution of *n*BuLi (2.5 M, 5.76 mL, 14.4 mmol) was added slowly by using a syringe to a solution of **7** (3 g, 7.48 mmol) in freshly distilled THF (150 mL) at −78°C under N_2. The resulting mixture was stirred at this temperature for 1 h. Then, DMF (5.76 mL, 74.7 mmol) was added and the mixture was stirred for another 1 h at −78°C. After this time, the mixture was gradually warmed to room temperature and stirred overnight. Saturated aqueous NH_4Cl (100 mL) was added. The mixture was extracted with dichloromethane (2×100 mL). The combined organic extracts were dried over anhydrous sodium sulfate, filtered, and the solvent was removed under reduced pressure. The residue was purified by flash chromatography on silica gel (dichloromethane) to afford product **8** (1.504 g, 67.2%). ^{1}H NMR (400 MHz, $CDCl_3$): δ=10.16 (s, 2H), 8.73 (s, 2H), 8.03 (d, J=8.5 Hz, 2H), 7.71 (t, J=7.4 Hz, 2H), 7.62 (t, J=7.4 Hz, 1H), 7.55 (d, J=7.3 Hz, 2H), 7.46 ppm (d, J=8.5 Hz, 2H); ^{13}C NMR (100 MHz, $CDCl_3$): δ=191.47, 145.36, 135.85, 130.42, 129.09, 128.13, 127.18, 124.13, 123.44, 110.88 ppm; MS (EI): m/z: 299 $[M]^+$; HRMS (GCT-MS): calcd for $C_{20}H_{13}NO_2$: 299.0946; found: 299.0944 $[M]^+$.

Compound 2: This compound was prepared according to the general procedure for **1** by using Zn (4.347 g, 66.9 mmol), $TiCl_4$ (3.62 mL, 33.4 mmol), **8** (1 g, 3.34 mmol), and pyridine (2.33 mL) in THF (300 mL). Column chromatography was performed on silica gel (dichloromethane) to get the crude product. This was then further purified by gradient sublimation. Compound **2** (about 50 mg, 5.6%) was obtained as a yellow solid. M.p. 363°C; ^{1}H NMR (400 MHz, $CDCl_3$): δ=9.80 (s, 4H), 7.65–7.58 (m, 8H), 7.52–7.46 (m, 2H), 7.29 (d, J=7.3 Hz, 4H), 7.19 (d, J=8.5 Hz, 4H), 6.43 (s, 4H); MS (EI): m/z: 534 $[M]^+$; HRMS (GCT-MS): calcd for $C_{40}H_{26}N_2$: 534.2096; found: 534.2103 $[M]^+$; elemental analysis calcd (%) for $C_{40}H_{26}N_2$: C 89.86, H 4.90, N 5.24; found: C 89.59, H 4.88, N 5.29.

9-*n*-Butyl-carbazole-3-carbaldehyde (9): This compound was prepared according to the general procedure for **5** by using 9-*n*-butylcarbazole (3.345 g, 13.33 mmol), phosphorus oxychloride (1.568 mL, 16.82 mmol), and DMF (1.319 mL, 19.50 mmol). The mixture was purified by flash chromatography on silica gel (50% dichloromethane in petroleum ether) to afford **9** (6.33 g, 66.9%). ^{1}H NMR (400 MHz, $CDCl_3$): δ=10.10 (s, 1H), 8.61 (s, 1H), 8.17 (d, J=7.8 Hz, 1H), 8.02 (d, J=8.5 Hz, 1H), 7.55 (t, J=7.8 Hz, 1H), 7.45 (t, J=7.4 Hz, 2H), 7.34 (t, J=7.4 Hz, 1H), 4.36 (t, J=7.2 Hz, 2H), 1.92–1.84 (m, 2H), 1.46–1.37 (m, 2H), 0.98 ppm (t, J=7.3 Hz, 3H); ^{13}C NMR (100 MHz, $CDCl_3$): δ=191.79, 144.05, 141.16, 128.46, 127.12, 126.71, 123.97, 123.02, 122.97, 120.73, 120.29, 109.42, 108.94, 43.16, 31.05, 20.53, 13.87 ppm; MS (EI): m/z: 251 $[M]^+$; HRMS (GCT-MS): calcd for $C_{17}H_{17}NO$: 251.1310; found: 251.1313 $[M]^+$.

Compound 3: This compound was prepared according to the general procedure for **1** by using Zn (5.18 g, 7.97 mmol), $TiCl_4$ (4.415 mL, 40.03 mmol), 9-*n*-butyl-carbazole-3-carbaldehyde (2 g, 7.97 mmol), and pyridine (5 mL) in THF (300 mL). Column chromatography was performed on silica gel (CH_2Cl_2/ petroleum ether 1:2) to give the crude product. Recrystallization from CH_2Cl_2/hexane gave **3** (1.086 g, 58.0%) as a jade-green powder. M.p. 207°C; ^{1}H NMR (400 MHz, $CDCl_3$): δ=8.28 (s, 2H), 8.16 (d, J=7.7 Hz, 2H), 7.74 (d, J=8.5 Hz, 2H), 7.49–7.40 (m, 6H), 7.37 (s, 2H), 7.26–7.23 (m, 2H), 4.34 (t, J=7.1 Hz, 4H), 1.92–1.85 (m, 4H), 1.47–1.38 (m, 4H), 0.98 ppm (t, J=7.3 Hz, 6H); ^{13}C NMR (100 MHz, $CDCl_3$): δ=129.21, 127.03, 125.69, 124.24, 123.22, 122.95, 120.45, 118.88, 118.26, 108.89, 108.84, 42.97, 31.20, 20.61, 13.94 ppm; MS (EI): m/z: 470 $[M]^+$; HRMS (GCT-MS): calcd for $C_{34}H_{34}N_2$: 470.2722; found: 470.2727 $[M]^+$; elemental analysis calcd (%) for $C_{34}H_{34}N_2$: C 86.77, H 7.28, N 5.95; found: C 87.00, H 7.44, N 6.06.

Acknowledgement

The authors are grateful for financial support from the National Natural Science Foundation of China (Grant Nos 20572113, 20632020, 20721061), the State Key Basic Research Program (2006CB9321001, 2006CB806201), and the Chinese Academy of Sciences.

[1] Y. Shirota, H. Kageyama, *Chem. Rev.* **2007**, *107*, 953.

[2] a) T. W. Kelley, P. F. Baude, C. Gerlach, D. E. Ender, D. Muyres, M. A. Haase, D. E. Vogel, S. D. Theiss, *Chem. Mater.* **2004**, *16*, 4413; b) Y. Sun, Y. Liu, D. Zhu, *J. Mater. Chem.* **2005**, *15*, 53; c) J. E. Anthony, *Chem. Rev.* 2006, 106, 5028; d) A. R. Murphy, J. M. J. Fréchet, *Chem. Rev.* **2007**, *107*, 1066; e) A. Facchetti, *Mater. Today* **2007**, 10, 28.

[3] a) H. Sirringhaus, T. Kawase, R. H. Friend, T. Shimoda, M. Inbasekaran, W. Wu, E. P. Woo, *Science* **2000**, *290*, 2123; b) Z. Bao, *Adv. Mater.* **2000**, *12*, 227; c) S. R. Forrest, *Nature* **2004**, *428*, 911; d) H. Sirringhaus, *Adv. Mater.* **2005**, *17*, 2411; e) M. Berggren, D. Nilsson, N. D. Robinson, *Nat. Mater.* **2007**, 3; f) E. Menard, M. A. Meitl, Y. Sun, J. U. Park, D. J. Shir, Y. S. Nam, S. Jeon, J. A. Rogers, *Chem. Rev.* **2007**, *107*, 1117.

[4] For example: a) Z. Wang, C. Kim, A. Facchetti, T. J. Marks, *J. Am. Chem. Soc.* **2007**, *129*, 13362; b) S. Handa, E. Miyazaki, K. Takimiya, Y. Kunugi, *J. Am. Chem. Soc.* **2007**, *129*, 11684; c) P.-L. T. Boudreault, S. Wakim, N. Blouin, M. Simard, C. Tessier, Y. Tao, M. Leclerc, *J. Am. Chem. Soc.* **2007**, *129*, 9125; d) H. Pan, Y. Li, Y. Wu, P. Liu, B. S. Ong, S. Zhu, G. Xu, *J. Am. Chem. Soc.* **2007**, *129*, 4112; e) M. Zhang, H. N. Tsao, W. Pisula, C. Yang, A. K. Mishra, K. Mullen, *J. Am. Chem. Soc.* **2007**, *129*, 3472; f) T. Yamamoto, K. Takimiya, *J. Am. Chem. Soc.* **2007**, *129*, 2224; g) T. Okamoto, M. L. Senatore, M.-M. Ling, A. B. Mallik, M. L. Tang, Z. Bao, *Adv. Mater.* **2007**, *19*, 3381; h) X. Gao, Y. Wang, X. Yang, Y. Liu, W. Qiu, W. Wu, H. Zhang, T. Qi, Y. Liu, K. Lu, C. Du, Z. Shuai, G. Yu, D. Zhu, *Adv. Mater.* **2007**, *19*, 3037; i) L. Li, Q. Tang, H. Li, X. Yang, W. Hu, Y. Song, Z. Shuai, W. Xu, Y. Liu, D. Zhu, *Adv. Mater.* **2007**, *19*, 2613.

[5] K. Takimiya, Y. Kunugi, T. Otsubo, *Chem. Lett.* **2007**, *36*, 578.

[6] a) J.-F. Morin, M. Leclerc, D. Adès, A. Siove, *Macromol. Rapid Commun.* **2005**, *26*, 761; b) J. V. Grazulevicius, P. Strohriegl, J. Pielichowski, K. Pielichowski, *Prog. Polym. Sci.* **2003**, *28*, 1297.

[7] For example: a) K. Brunner, A. Dijken, H. Börner, J. J. A. M. Bastiaansen, N. M. M. Kiggen, B. M. W. Langeveld, *J. Am. Chem. Soc.* **2004**, *126*, 6035; b) M. H. Tsai, Y. H. Hong, C. H. Chang, H. C. Su, C. C. Wu, A. Matoliukstyte, J. Simokaitiene, S. Grigalevicius, J. V. Grazulevicius, C. P. Hsu, *Adv. Mater.* **2007**, *19*, 862; c) Y.-C. Chen, G.-S. Huang, C.-C. Hsiao, S.-A. Chen, *J. Am. Chem. Soc.* **2006**, *128*, 8549.
[8] Y. Zhang, T. Wada, H. Sasabe, *J. Mater. Chem.* **1998**, *8*, 809.
[9] a) J.-F. Morin, N. Drolet, Y. Tao, M. Leclerc, *Chem. Mater.* **2004**, *16*, 4619; b) Y. Wu, Y. Li, S. Gardner, B. S. Ong, *J. Am. Chem. Soc.* **2005**, *127*, 614; c) Y. Wu, Y. Li, S. Gardner, B. S. Ong, *Adv. Mater.* **2005**, *17*, 849; d) N. Drolet, J.-F. Morin, N. Leclerc, S. Wakim, Y. Tao, M. Leclerc, *Adv. Funct. Mater.* **2005**, *15*, 1671; e) M. Sonntag, K. Kreger, D. Hanft, P. Strohriegl, S. Setayesh, D. De Leeuw, *Chem. Mater.* **2005**, *17*, 3031.
[10] For recent reviews, see: a) J. S. Moore, *Acc. Chem. Res.* **1997**, *30*, 402; b) S. Höger, *J. Polym. Sci., Part A: Polym. Chem.* **1999**, *37*, 2685; c) M. M. Haley, J. J. Pak, S. C. Brand, *Top. Curr. Chem.* **1999**, *201*, 81; d) C. Grave, A. D. Schlüter, *Eur. J. Org. Chem.* **2002**, 3075; e) D. Zhao, J. S. Moore, *Chem. Commun.* **2003**, 807; f) Y. Yamaguchi, Z. I. Yoshida, *Chem. Eur. J.* **2003**, *9*, 5430; g) S. Höger, *Chem. Eur. J.* **2004**, *10*, 1320; h) *Acetylene Chemistry*, (Eds.: F. Diederich, P. J. Stang, R. R. Tykwinsky), Wiley-VCH, Weinheim, **2005**; i) W. Zhang, J. S. Moore, *Angew. Chem.* **2006**, *118*, 4524; *Angew. Chem. Int. Ed.* **2006**, *45*, 4416.
[11] P. Bäuerle, *Adv. Mater.* **1992**, *4*, 102.
[12] a) S. Maruyama, Y. D. Zhang, T. Wada, H. Sasabe, *J. Chem. Soc. Perkin Trans. 1* **1999**, 41; b) S. Maruyama, X. T. Tao, H. Hokari, T. Noh, Y. D. Zhang, T. Wada, H. Sasabe, H. Suzuki, T. Watanabe, S. Miyata, *J. Mater. Chem.* **1999**, *9*, 893; c) S. Maruyama, H. Suzuki, X. T. Tao, T. Wada, H. Sasabe, S. Miyata, T. Kamata, *Phys. Chem. Chem. Phys.* **2000**, *2*, 3565; d) S. Maruyama, H. Hokari, X. T. Tao, A. Gunji, T. Wada, H. Sasabe, *Chem. Lett.* **1999**, 731; e) W. Zhang, J. S. Moore, *J. Am. Chem. Soc.* **2004**, *126*, 12796.
[13] T. Naddo, Y. Che, W. Zhang, K. Balakrishnan, X. Yang, M. Yen, J. Zhao, J. S. Moore, L. Zang, *J. Am. Chem. Soc.* **2007**, *129*, 6978.
[14] K. Balakrishnan, A. Datar, W. Zhang, X. Yang, T. Naddo, J. Huang, J. Zuo, M. Yen, J. S. Moore, L. Zang, *J. Am. Chem. Soc.* **2006**, *128*, 6576.
[15] T. Zhao, Z. Liu, Y. Song, W. Xu, D. Zhang, D. Zhu, *J. Org. Chem.* **2006**, *71*, 7422.
[16] a) Y. Song, C. Di, X. Yang, S. Li, W. Xu, Y. Liu, L. Yang, Z. Shuai, D. Zhang, D. Zhu, *J. Am. Chem. Soc.* **2006**, *128*, 15940; b) Y. Song, C. Di, W. Xu, Y. Liu, D. Zhang, D. Zhu, *J. Mater. Chem.* **2007**, *17*, 4483.
[17] J. Roncali, *Chem. Rev.* **1997**, *97*, 173.
[18] J. Ostrauskaite, V. Voska, J. Antulis, V. Gaidelis, V. Jankauskas, J. V. Grazulevicius, *J. Mater. Chem.* **2002**, *12*, 3469.
[19] a) J. E. McMurry, *Chem. Rev.* **1989**, *89*, 1513; b) Z. Hu, J. L. Atwood, M. P. Cava, *J. Org. Chem.* **1994**, *59*, 8071.
[20] M. Thelakkat, H.-W. Schmidt, *Adv. Mater.* **1998**, *10*, 219.
[21] X. Gao, W. Wu, Y. Liu, S. Jiao, W. Qiu, G. Yu, L. Wang, D. Zhu, *J. Mater. Chem.* **2007**, *17*, 736.
[22] M. Bednarza, P. Reinekera, E. Mena-Osteritzb, P. Bäuerle. *J. Luminescence* **2004**, *110*, 225.
[23] a) N. F. Mott, E. A. Davis, *Electronic Processes in Non-Crystalline Materials*, 2nd ed., Oxford University Press, Oxford, **1979**; b) J. A. Reedijk, H. C. F. Martens, S. M. C. van Bohemen, O. Hilt, H. B. Brom, M. A. J. Michels, *Synth. Met.* **1999**, *101*, 475; c) A. J. Epstein, W. P. Lee, V. N. Prigodin, *Synth. Met.* **2001**, *117*, 9.
[24] a) R. A. Marcus, *Rev. Mod. Phys.* **1993**, *65*, 599; b) N. E. Gruhn, D. A. da Silva Filho, T. G. Bill, M. Malagoli, V. Coropceanu, A. Kahn, J.-L. Brédas, *J. Am. Chem. Soc.* **2002**, *124*, 7918; c) J. L. Brédas, J. P. Calbert, D. A. da Silvo Filho, J. Cornil, *Proc. Natl. Acad. Sci. USA* **2002**, *99*, 5804.
[25] G. R. Hutchison, M. A. Ratner, T. J. Marks, *J. Am. Chem. Soc.* **2005**, *127*, 2339.
[26] a) S. W. Cha, J. I. Jin, *J. Mater. Chem.* **2003**, *13*, 479; b) M. Park, J. R. Buck, C. J. Rizzo, *Tetrahedron* **1998**, *54*, 12707.
[27] Gaussian 03 (Revision B.05), M. J. Frisch, G. W. Trucks, H. B. Schlegel, G. E. Scuseria, M. A. Robb, J. R. Cheeseman, J. A. Montgomery, Jr., T. Vreven, K. N. Kudin, J. C. Burant, J. M. Millam, S. S. Iyengar, J. Tomasi, V. Barone, B. Mennucci, M. Cossi, G. Scalmani, N. Rega, G. A. Petersson, H. Nakatsuji, M. Hada, M. Ehara, K. Toyota, R. Fukuda, J. Hasegawa, M. Ishida, T. Nakajima, Y. Honda, O. Kitao, H. Nakai, M. Klene, X. Li, J. E. Knox, H. P. Hratchian, J. B. Cross, C. Adamo, J. Jaramillo, R. Gomperts, R. E. Stratmann, O. Yazyev, A. J. Austin, R. Cammi, C. Pomelli, J. W. Ochterski, P. Y. Ayala, K. Morokuma, G. A. Voth, P. Salvador, J. J. Dannenberg, V. G. Zakrzewski, S. Dapprich, A. D. Daniels, M. C. Strain, O. Farkas, D. K. Malick, A. D. Rabuck, K. Raghavachari, J. B. Foresman, J. V. Ortiz, Q. Cui, A. G. Baboul, S. Clifford, J. Cioslowski, B. B. Stefanov, G. Liu, A. Liashenko, P. Piskorz, I. Komaromi, R. L. Martin, D. J. Fox, T. Keith, M. A. Al-Laham, C. Y. Peng, A. Nanayakkara, M. Challacombe, P. M. W. Gill, B. Johnson, W. Chen, M. W. Wong, C. Gonzalez, J. A. Pople, Gaussian, Inc., Pittsburgh PA, **2003**.

Received: January 3, 2008
Published online: April 2, 2008

